

Structural and thermal properties of nickel oxide nanoparticles doped cadmium zinc borate glasses: preparation and characterization

E. A. Allam ^{a,b}, R. M. El-Sharkawy ^{c,*}, Kh.S. Shaaban ^d, A. El-Taher ^e,
M. E. Mahmoud ^a, Y. El Sayed ^f

^aAlexandria University, Faculty of Science, Chemistry Department, P.O. Box 426, Ibraheimia 21321, Alexandria, Egypt.

^bMinistry of Health and Population, Central Labs of Alexandria, P.O. Box 21518, Alexandria, Egypt.

^cChemistry Department, Faculty of Dentistry, Pharos University in Alexandria, P.O. Box 37, Sidi Gaber, Alexandria, Egypt.

^dChemistry Department, Faculty of Science, Al-Azhar University, Assiut, 71524, Egypt

^ePhysics Department, Faculty of Science, Al-Azhar University, Assuit Branch, 71524 Assuit, Egypt

^fPhysics Dep., Faculty of Science, King Khalid University, P. O. Box 9004, Abha, Saudi Arabia

Nickel-doped cadmium zinc borate glass of various nickel oxide content was prepared as $x\text{NiO}-20\text{ZnO}-60\text{B}_2\text{O}_3-(20-x)\text{CdO}$ ($0 \leq x \leq 5$ mol %), by the melt quenching method based on nano metal oxides. Both the zinc oxide nanoparticles (ZnO NPs) and cadmium oxide nanoparticles (CdO NPs) were prepared via the solution-combustion technique. Nickel oxide nanoparticles (NiO NPs) was synthesized by the combustion of $\text{Ni}(\text{OH})_2$ and boron oxide nanoparticles (B_2O_3 NPs) was synthesized by the solid-state reaction method. The amorphous nature of these types of glass was confirmed using X-ray diffraction analysis (XRD). The morphology of nano-metal oxides was investigated via the scanning electron microscope (SEM). SEM imaging showed that the NiO NPs had a semi-spherical morphology, and that their average particle size was 22.17 nm. The Fourier-transform infrared spectroscopy's (FTIR) spectral analysis was used to identify the structural units of these types of glass via deconvolution, in terms of multi-Gaussian fitting. Results proved that Ni^{4+} plays an important role and a key to improve the formation of the BO_4 network units. Finally, the high thermal stability and glass transition temperature of the prepared glass samples were increased by increasing the loading of NiO NPs from 0.0 mol % - 5.0 mol % and this was established by using DTA.

(Received October 3, 2021; Accepted February 2, 2022)

Keywords: Nano metal oxides, SEM, Glasses, IR, DTA

1. Introduction

Recently, nanotechnology has been established as a simple and modern technology to improve the quality of various products, with strong emphasis on diverse applications, including water treatment and others in the petrochemical industry, medicine, catalysis, and energy. It is possible to find nanotechnology in medicine, food, cars, and paints used in houses, hence the importance of this technology in our daily life. Metal oxides have had a lot of applications in numerous industries, in recent decades. The demand for the synthesis of metal oxides in nano form has increased, because of their unique properties, as well as their high efficiency during industrial applications, such as glass fabrication. Glass fabricated from nano metal oxides has great importance, because it is used in many fields, such as healthcare, the nuclear industry and other fields [1,2]. Nickel oxide in the form of nanoparticles is an important type of oxide, because it is used in the anode layer of solid oxide fuel cells, ceramic structures, cathodes for lithium ion micro

* Corresponding author: atef.eltaher@gmail.com
<https://doi.org/10.15251/DJNB.2022.171.161>

batteries, optical filters, smart windows, and in sensors [3-5]. Glass containing nickel oxide has excellent durability, optical density, chemical stability and numerous industrial possibilities [6]. Borate glass is a strong glass former, having three or four coordination numbers, with BO_3 or BO_4 as structure units. These structural units are interconnected through B-O-B bonds, which enhance the chemical and physical properties of these types of glass [7-11]. Borate glass doped with a heavy metal oxide (HMO), such as CdO, has enhanced properties [12]. Glass can be doped with transition metal ions (TMIs), like nickel, which has more than one valence state, giving it good optical/electrical properties [13]. Nickel oxide can color the host glass matrix, when added in small amounts, because it occupies the glass matrix and is a capable modifier and network former [14-15]. The study of the different properties of glass containing bismuth borate with Ni^{2+} has been established. It has been concluded that Ni^{2+} has emission centers and is optically active [16]. Physical and chemical properties of borate glass doped with nickel ions were studied and the formation of BO was observed. These modifications show Ni^{2+} ions as network formers [17-20]. For intense, Thakur et al. [21] investigated the physical and thermal properties of Nickel doped Bismuth Borate glasses with composition $(70\text{B}_2\text{O}_3-(30-x)\text{Bi}_2\text{O}_3-x\text{NiO})$ where $x=0, 0.5, 1.0, 1.5, 2.0$ (wt%). The conclusion they reached from the DTA and OPD data that as the Ni content increased in the glass system, its glass transition temperature (T_g) decreased. In addition, they found from the FTIR and Raman studies that the glass network mainly comprises of $[\text{BiO}_3]$, $[\text{BiO}_6]$, $[\text{BO}_3]$ and $[\text{BO}_4]$ units. Sallam et al. [22] studied the physical properties and radiation shielding parameters of bismuth borate glasses doped 0.7 % of Cu, Co, Ni transition metals Cu, Co, Ni and the results showed that both band gap and electronegativity decreased by the addition of these transition metals. Mahapatra et al. [23] studied the effects of nickel replacement of glass formers SiO_2 and B_2O_3 and glass modifier SrO on $\text{SrO-La}_2\text{O}_3\text{-Al}_2\text{O}_3\text{-B}_2\text{O}_3\text{-SiO}_2$ glass network structure and thermal properties. They found that the addition of nickel degrades glass thermal stability by increasing the amount of non-bridging oxygen atoms and devitrification. Cizman et al. [24] tested the activity of Ni in inorganic sodium borosilicate glasses doped with nickel oxide and they concluded that nano clusters of nickel oxides strongly affect structure and physical properties of sodium borosilicate (SBS) glasses. The effect of transition-metal ions (Ni^{2+} , Cu^{2+} and Co^{2+}) doping on the electric and dielectric properties the zinc Sodium phosphate glass was investigated by Kalai et al. [25]. They found that the changes in the conductivity and activation energy depend on the chemical composition of the glass sample and indicate a changeover of the predominant conduction mechanism from ionic to polaronic. As per Abul-Magd et al. [26] addition of NiO was found to improve the structural and optical properties of Nickel-doped sodium zinc borate (NZB) glass systems of composition $[15\text{ZnO}-(65-x)\text{B}_2\text{O}_3-x\text{NiO}-20\text{Na}_2\text{O}]$, where ($x = 0.0, 0.5, 1.0, 1.5, 2.0, 2.5$ and 3.0 mol %) based on concluded results.

In this work, CdO, ZnO, B_2O_3 , and NiO, nano metal oxides have been synthesized to prepare glass with the composition, $x\text{NiO}-20\text{ZnO}-60\text{B}_2\text{O}_3-(20-x)\text{CdO}$ ($0 \leq x \leq 5$ mol %). Thus, the influence of nickel oxide NPs on the structure and thermal characteristics of the formed glass samples has been established.

2. Experimental

2.1. Synthesis of Nano Metal Oxides

2.1.1. Synthesis of (ZnO NPs)

To prepare ZnO NPs, a simple combustion technique was implemented [27]. 100 mL of 0.5 M of NaOH was mixed with 500 mL of 0.05 M of $\text{Zn}(\text{CH}_3\text{COO})_2 \cdot 2\text{H}_2\text{O}$ at a temperature of 60°C in a standard experimental procedure. The mixture was heated to 80°C , with 90 minutes of continuous stirring. Then, as a white precipitate, $\text{Zn}(\text{OH})_2$ was acquired. The prepared $\text{Zn}(\text{OH})_2$ was collected by decantation, washed with deionized water and dried for 24 hrs at 70°C . The suitable stoichiometric amounts of precipitate and glycine ($\text{NH}_2\text{-CH}_2\text{-COOH}$) were mixed in deionized water following this stage, while stirring at 80°C , until a paste was created. This paste was dried for 24 hrs at 70°C and finally heated for 6 hrs to 900°C to obtain ZnO NPs.

2.1.2. Synthesis of (CdO NPs)

CdO NPs were prepared using the solution–combustion synthesis. A molar ratio, [1.8 g of urea ($\text{CO}(\text{NH}_2)_2$) and 15.42g of cadmium nitrate tetrahydrate ($\text{Cd}(\text{NO}_3)_2 \cdot 4\text{H}_2\text{O}$)] as precursors, was added to 5 mL of deionized water. Following this step, calcination at 750°C for 6 hrs took place [28]. The combustion reaction equation can be written as in Eq. (1):



In this reaction (solution–combustion), CdO powder was obtained, also CO_2 , N_2 , and H_2O molecules were released, to generate porous CdO, as fine particles with a spherical shape. This was confirmed by SEM imaging. In this reaction, urea acted as a fuel and H_2O had an important role in the formation of the porous structure of CdO powder, via the exothermic reaction that occurred [29].

2.1.3. Synthesis of NiO NPs

NiO NPs were prepared via the combustion synthesis of $\text{Ni}(\text{OH})_2$ [30]. $\text{Ni}(\text{OH})_2$ was prepared after 0.1 M nickel chloride hexahydrate ($\text{NiCl}_2 \cdot 6\text{H}_2\text{O}$) was dissolved in ethanol. Following this step, the mixture was added to a hydrazine monohydrate solution (6.73 ml of molar ratio 5). The reaction's pH was between 8.0–12.0, using NaOH. The reactants were stirred for 90 min at standard room temperature. The product was then washed with deionized water to remove reaction residues, then with acetone. Finally, green $[\text{Ni}(\text{OH})_2 \cdot 0.5\text{H}_2\text{O}]$ nanoparticles were obtained and dried in an oven at 70°C for 24 hrs. NiO NPs were obtained via the combustion of nickel hydroxide nanoparticles at 850°C .

2.1.4. Synthesis of (B_2O_3 NPs)

B_2O_3 NPs were synthesized at $200\text{--}250^\circ\text{C}$ in ambient air by the solid-state reaction of boric acid and urea. Next, the dry mixture of boric acid with urea was 4:1 in a molar ratio. The mixed powders were then heated in a preheated muffle furnace for 60 min at 200°C , then for 120 min at 250°C . Finally, using an agate pestle and a mortar, the resulting product was ground into powder.

2.2. Glass Fabrication and its Characterization

The assembled glass samples were fabricated via the melt quenching method as per the procedure discussed by El-Sharkawy et al [8]. These were investigated by XRD and FTIR and their thermal stability was estimated. In such experimental procedure, the pure powder of NiO NPs, CdO NPs, B_2O_3 NPs and ZnO NPs were pulverized together to obtain a mixture for each glass sample. The produced powder mixture was then melted in an electrically heated furnace at about 1423 K in regular atmospheric pressure in Pt crucibles, for 4 hrs to homogenize the melt, which was then added to a preheated mold. This mold was moved right away to a different furnace heated to 740 K for two hours to anneal the glass. Table 1 shows the chemical composition (mol %) of the starting mixtures of the prepared glass samples with the chemical formula $x\text{NiO} - 20\text{ZnO} - 60\text{B}_2\text{O}_3 - (20-x)\text{CdO}$ ($0 \leq x \leq 5$ mol %).

Table 1. Chemical composition of the prepared glass samples (mol %).

Sample Name	Chemical Composition (mol %)			
	CdO NPs	ZnO NPs	B_2O_3 NPs	NiO NPs
G 1	20	20	60	0
G 2	19	20	60	1
G 3	18	20	60	2
G 4	16	20	60	4
G 5	15	20	60	5

3. Results and Discussion

3.1. Scanning Electron Microscope for Nano-Metal Oxides

Fig. 1a displays the morphology of the CdO nanocrystallites. From this figure, it is clearly observed that with some aggregates, the CdO NPs exist as near spherical-shape particles with some aggregates. The particle dimensions were identified to be in the 16.67–33.33 nm range. Fig. 1b displays the SEM picture of ZnO NPs and the distribution of their particle size. It is clearly observed that the nanoparticles, because of the presence of agglomerations, were spread over a wide area. Fig. 1c displays the SEM image of the B₂O₃ NPs in Fig. 1c. It can be seen that the synthesized B₂O₃ nanoparticles have semi-spherical shape. The particle size of B₂O₃ NPs was identified to fall within the range of 31.30–70.71 nm, which confirms its nanoscale structure. Some coalesced nanoparticles were also seen. The SEM image and particle size distribution of the NiO NPs are shown in Fig. 1d. The SEM image showed that the NiO NPs have a semi-spherical morphology, and that their average particle size is 22.17 nm.

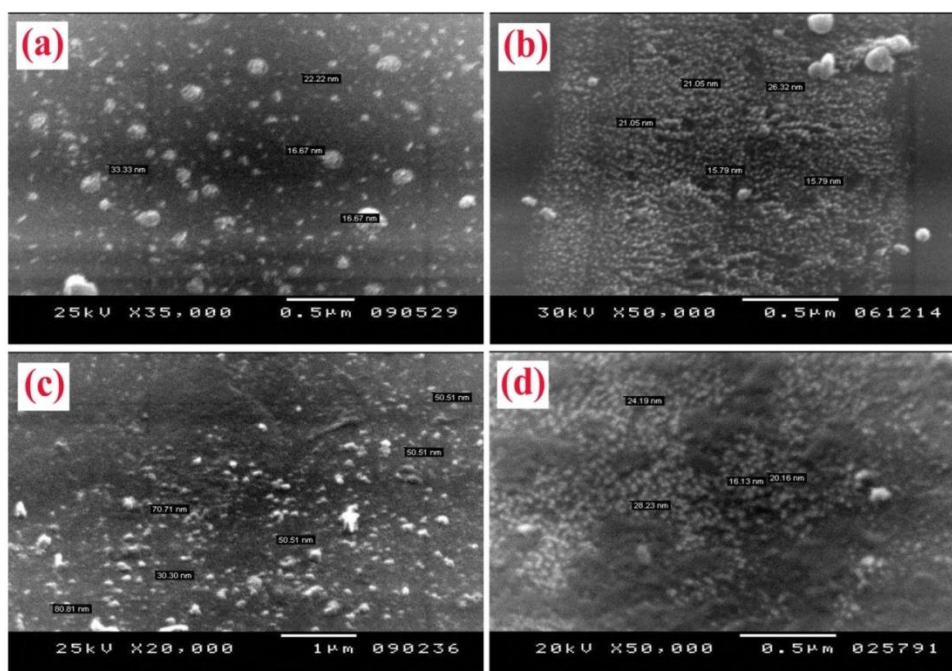


Fig.1 SEM-images of (a) CdO NPs, (b) ZnO NPs, (c) B₂O₃ NPs and (d) NiO NPs.

3.2. FTIR Spectroscopy of the Prepared Glass Samples

The FTIR analysis is a suitable technique for studying the structural units of the glass samples. The IR spectra of NiO glass network are depicted in Fig.2, and their peak assignments are given in Table 2. The deconvolution of the glass samples took place using Gaussian fitting and can be seen in symmetrical peaks at around 512–596 cm⁻¹, 680–692 cm⁻¹, 855–897 cm⁻¹, 962–997 cm⁻¹, 1064–1077 cm⁻¹, and 1252–1411 cm⁻¹. They are shown in Figs.3, 4, and 5.

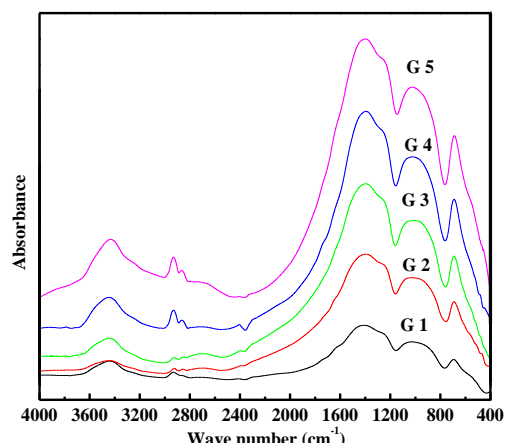


Fig.2 FT-IR spectra for the investigated glass samples.

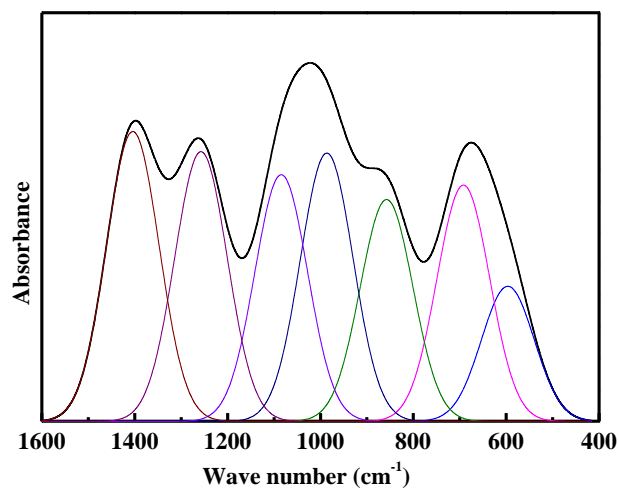


Fig.3 Curve-fitting of the IR spectra of glass samples G 1.

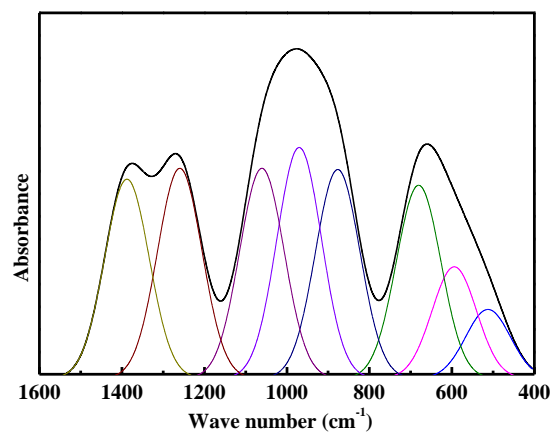


Fig.4 Curve-fitting of the IR spectra of glass samples G 3.

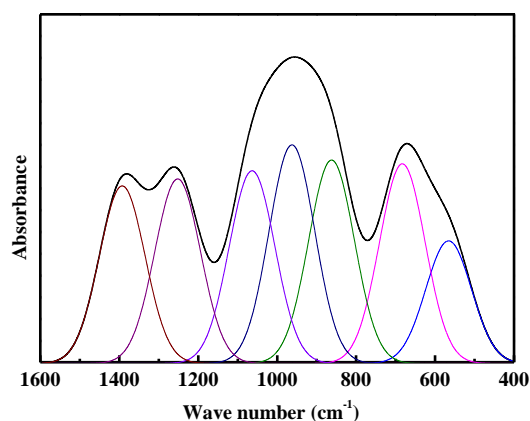


Fig.5 Curve-fitting of the IR spectra of glass samples G 5.

These bands are listed in Table 2. The band at 512-596 cm^{-1} is related to the bending vibrations of (ZnO_6) and (CdO_6) . There is also an overlap between the vibrations of $\text{Zn}-\text{O}$ and the bending vibrations of the (BO_3) units [31-39]. The vibration of the $\text{Ni}-\text{O}-\text{Ni}$ linkages appears at the band between 680 and 692 cm^{-1} [6]. The vibrations of the $[\text{BO}_4]$ structural group appear in the band between 855 and 1077 cm^{-1} . There seems to be certain shifts in the wave number, which could be due to the increase in the $[\text{BO}_4]$ units in the glass network. The vibrations of the $[\text{BO}_3]$ units with and without non-bridging oxygen appear in the 1252–1411 cm^{-1} band range. The fraction (N_4) is calculated from Eq. (2) by considering the assignments in Table 2 and the area under the bands.

$$N_4 = \frac{BO_4}{(BO_4 + BO_3)} \quad (2)$$

Table 2. Attribution of deconvoluted IR absorption peaks of the studied glass samples.

Wave Number (cm^{-1})	Assignment
512-596	Is related to the bending vibrations of (ZnO_6) and (CdO_6) units
680-692	Is due to the vibration of the $\text{Ni}-\text{O}-\text{Ni}$ linkages
855-1077	Is attributed to the vibrations of the $[\text{BO}_4]$ units in various structural groups
1252-1411	Is attributed to the vibrations of $[\text{BO}_3]$ structural units with and without non-bridging oxygen

The value of the N_4 fraction has witnessed an increase, since the oxygen environment has become richer and the creation of more $[\text{BO}_4]$ structural units has increased, and the bonding of nickel borate glass has become stronger. This has led to a stronger glass network, subsequently; the ring type structure of borate glass has become packed, through matrix polymerizations. A short report about the deconvolution parameters of the infrared spectra of the investigated glass samples are shown in Table3.

Table 3. Deconvolution parameters of the infrared spectra of studied glass samples, where (C) is the band center and (A) is the relative area (%) of the component band and N_4

G 1	C	-	565.7	682.9	862.2	962.6	1064	1252	1392	-	BO ₄	BO ₃	N ₄
	A	-	9.414	15.37	15.67	16.83	14.84	14.21	13.67	-	47.33	27.88	48.33
G 2	C	-	563.4	692.2	897.6	993.3	1061	1269	-	1411			
	A	-	8.334	13.76	15.43	16.52	15.18	14.43	-	16.35	47.13	30.78	48.13
G 3	C	-	568	685.2	855.2	986.4	1077	1271	1379	-			
	A	-	7.198	14.05	14.86	16.98	15.18	16.31	15.42	-	47.02	31.73	48.02
G 4	C	512.3	594.2	680.6	876.7	970.1	1061	1260	1388	-			
	A	4.714	7.795	13.5	14.59	16.13	14.68	14.68	13.92	-	45.4	28.59	46.4
G 5	C	-	596.5	692.2	857.6	986.4	1084	1257	-	1404			
	A	-	8.098	14.17	13.3	16.09	14.79	16.17	-	17.38	44.18	33.55	45.18

3.3. X-Ray Diffraction of the Prepared Glass

Measurements of X-ray diffraction were established to confirm that the prepared glass samples have amorphous structure. Fig. 6 shows the X-ray patterns of the samples. The XRD curves show broad peaks and indiscrete lines, which indicate the high degree of glassy state of the samples. The halo broadness differed for all glass samples, but all of them did not show any trace within the crystalline phase. The amorphous state was confirmed by the continuous diffraction pattern with no sharp peak and the broad peak centered on $2\theta = 30^\circ$. The peak broadening can be attributed to its amorphous structure. A small shift in the broad hump at $2\theta = 30^\circ$ values due to NiO content, which increased the coordination number of oxygens while decreasing bond length.

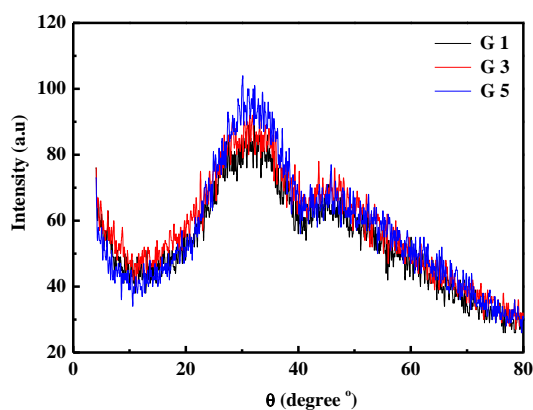


Fig.6 XRD patterns of the selected glass samples.

3.4. Differential Thermal Analysis (DTA)

The thermal behaviours of prepared glasses characterized by DTA at a heating rate (10°C/min). The function temperatures (T_g , T_c , T_p , and T_m) of the prepared glass samples have been determined using DTA [39, 40]. Fig. 7 shows the DTA thermogram of cadmium zinc borate glass samples with different mol% of nickel oxide NPs (20-x)CdO–20ZnO–60B₂O₃–xNiO (0 ≤ x ≤ 5 mol %). The thermographs of DTA give the value of (T_g) the temperature of glass transition in the endothermic process, (T_c) the temperature of crystallization in the exothermic process, and the value of (T_p) the peak crystallization temperature [42]. The calculations of the values of these temperatures are shown in Table 4. It was observed that the values of T_g , T_c and T_p increased with the increasing NiO NPs content in the glass system. Wang et al. have stated that the temperature of

glass transition (T_g) and temperature of crystallization (T_c) decrease with increasing the percent of NiO in the glass matrix [42]. The opposite trend was observed in this study of Ni doped cadmium zinc borate glass samples.

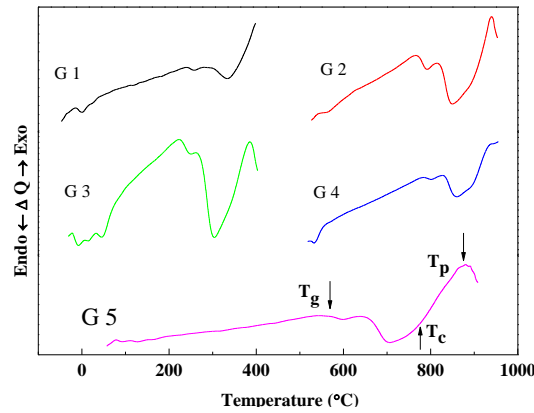


Fig. 7. DTA thermogram of the investigated glass samples.

From DTA curves it noticed that the values of T_g , T_c , and T_p increased with increasing NiO. This increase in the values of can be further justified by the following factors:

(1) The increasing formation of the bridging oxygen atoms, which are present in the matrix of glass, according to IR analysis.

(2) The permutation of Zn–O with Ni–O linkages; the Zn–O bond strength is (73 kcal/mol), which is weaker than the Ni–O bond strength, which is about (91.3 kcal/mol) [43]. This results in the increasing values of T_g , T_c , and T_p .

(3) The increase in the average force constant, as well as the crosslink densities.

In addition, the thermal stability parameter $\Delta T = T_c - T_g$ has been calculated for the prepared glass samples and is listed in Table 4. The values of ΔT increase with the increase in NiO NPs content; so, the thermal stability of the glass samples increases with the increase in NiO NPs content [44]. The other two criteria related to thermal stability are $H_g = \frac{\Delta T}{T_g}$ and

$$\Delta S = \frac{(T_p - T_c)\Delta T}{T_g} [44].$$

It was found that all thermal stability parameter values increase by adding NiO NPs in the glass matrix.

Table 4. Thermal parameter values of the studied glass samples.

Sample name	T_g	T_c	T_p	ΔT	ΔS	$T_p - T_c$	H_g
G 1	545	724	809	179	0.33	85	27.92
G 2	547	731	879	184	0.34	148	49.78
G 3	558	729	872	171	0.31	143	43.82
G 4	566	751	881	185	0.33	130	42.49
G 5	570	787	888	217	0.38	101	38.45

4. Conclusions

This study has explored the manufacturing of cadmium zinc borate glass, modified with NiO. All the materials for this purpose were in nano size. The physical aspects of these glass samples were characterized by FTIR, XRD, and SEM. As for the samples' thermal properties, they

were also investigated. As per the FTIR data, there is a transformation of BO_3 into BO_4 , which increases network connectivity within the glass samples. The glass transition temperature (T_g) and thermal stability (ΔT) increase with the increasing mol % of NiO NPs in the assembled glass samples (the value of T_g increased from 545 to 570°C and the value of ΔT increased from 179 to 217°C as the mol % of NiO NPs increased from 0.0 to 5.0).

These increases were attributed to the increase in the bond strength, the increase in the number of bridging oxygen atoms in the glass matrix, and the increase of the average force constant. In addition, the value of the other two parameters related to thermal stability (H_g and ΔS) were found to increase from 27.92 to 38.45 and from 0.33 to 0.38, respectively, as the NiO NPs content increased from 0.0 mol %-5.0 mol % in the glass matrix. Finally, it can be concluded that introducing NiO NPs at the expense of ZnO NPs in cadmium borate glass samples increases network connectivity.

Acknowledgments

The authors extend their appreciation to the Deanship of Scientific Research at King Khalid University (KKU) for funding this research project Number (R.G.P2/63/40).

References

- [1] J. Al Boukhari, A. Khalaf, R.S. Hassan, R. Awad, Appl. Phys. A126,323 (2020); <https://doi.org/10.1007/s00339-020-03508-3>
- [2] A.C. Gandhi, T.S. Chan, J. Pant, S.Y. Wu, Nanoscale Res. Lett. 12,207 (2017); <https://doi.org/10.1186/s11671-017-1988-x>
- [3] E. Erdem, K. Kiraz, M. Somer, R.A. Eichel, J. Eur. Ceram. Soc.30,289 (2010); <https://doi.org/10.1016/j.jeurceramsoc.2009.04.034>
- [4] J. Junaidi, M. Yunus, H. Harsojo, E. Suharyadi, K. Triyana, J. Adv. Sci. Eng. Inf. Technol.6,365 (2016); <https://doi.org/10.18517/ijaseit.6.3.808>
- [5] C. Mrabet, M. Ben Amor, A. Boukhachem, M. Amlouk, T. Manoubi, Ceram. Int.42,5963 (2016); <https://doi.org/10.1016/j.ceramint.2015.12.144>
- [6] S. Thakur, V. Thakur, A. Kaur, L. Singh, J. Non-Cryst. Solids 512, 60 (2019); <https://doi.org/10.1016/j.jnoncrysol.2019.02.012>
- [7] V.P. Singh, N.M. Badiger, Glass Phys. Chem. 41, (2762015).
- [8] R.M. El-Sharkawy, Kh.S. Shaaban, R. Elsamani, E.A. Allam, A. El-Taher, M.E. Mahmoud, J. Non-Cryst. Solids 528,119754 (2020); <https://doi.org/10.1016/j.jnoncrysol.2019.119754>
- [9] R. M El-Sharkawy, Elhassan A Allam, Atef El-Taher, Esam Ramadan Shaaban, Mohamed E Mahmoud., International Journal of Energy Research. 45,6, 8942-8959.(2021); <https://doi.org/10.1002/er.6427>
- [10] L. Baia, R. Stefan, W. Kiefer, J. Popp, S. Simon, J. Non-Cryst. Solids303,379 (2002); [https://doi.org/10.1016/S0022-3093\(02\)01042-6](https://doi.org/10.1016/S0022-3093(02)01042-6)
- [11] M. Farouk, A. Samir, F. Metawe, M. Elokr, J. Non-Cryst. Solids14, 371 (2013); <https://doi.org/10.1016/j.jnoncrysol.2013.04.001>
- [12] C. Stehle, C. Vira, D. Hogan, S. Feller, M. Aatigato, Phys. Chem. Glasses 39,83 (1998).
- [13] A.H. Hammad, A.M. Abdelghany, A. Okasha, S.Y. Marzouk, J. Mater. Sci.28,8662 (2017); <https://doi.org/10.1007/s10854-017-6590-6>
- [14] S. Suresh, T. Narendrudu, A.S. Kumar, M.V.S. Rao, G.C. Ram, D.K. Rao, Opt. Mater.60,67 (2016); <https://doi.org/10.1016/j.optmat.2016.07.012>
- [15] P.V. Rao, G.N. Raju, P.S. Prasad, C. Laxmikanth, N. Veeraiah, OptiK127,2920 (2016); <https://doi.org/10.1016/j.ijleo.2015.12.056>
- [16] M.S. Dahiya, S. Khasa, A. Agarwal, Phys. Chem. Glasses57,45 (2016); <https://doi.org/10.13036/17533562.57.2.023>
- [17] F.A. Moustafa, A.M. Fayad, F.M. Ezz-Eldin, I. El-Kashif, J. Non-Cryst. Solids.376,18 (2013); <https://doi.org/10.1016/j.jnoncrysol.2013.04.052>
- [18] A. Thulasiramudu, S. Buddhudu, J. Quant. Spect. Radiat. Transfer102,212 (2006); <https://doi.org/10.1016/j.jqsrt.2006.02.006>
- [19] H.B. Rudramadevi, S. Buddhudu, Ferroelectr. Lett. 36,82 (2009).
- [20] V.P. Singh, N.M. Badiger, Glass Phys. Chem. 41, 276 (2015); <https://doi.org/10.1134/S1087659615030177>

- [21]S. Thakur, V. Thakur, A. Kaur, L. Singh, J. Non-Cryst. Solids. 512,60 (2019); <https://doi.org/10.1016/j.jnoncrysol.2019.02.012>
- [22]O.I. Sallam,A.M. Madbouly,N.A. Elalaily,F.M. Ezz-Eldin, J. Alloys Compd. 843,156056 (2020); <https://doi.org/10.1016/j.jallcom.2020.156056>
- [23]M.K. Mahapatra, K. Lu, J. Power Sources 185,993 (2008); <https://doi.org/10.1016/j.jpowsour.2008.09.006>
- [24]A. Cizman, K. Idczak, M. Krupinski, M. Girsova, A. Zarzycki, E.R. Pasek, E. Zielony, P. Staniorowski, P. Wrzesinska, I. Perlikowski, E. Jach, L. Ermakova, T. Antropova, Comprehensive studies of activity of Ni in inorganic sodium borosilicate glasses doped with nickel oxide, (2021); <https://doi.org/10.1016/j.apsusc.2021.149891>
- [25]C. Kalaia, M. Kharroubia, L. Gacem, S. Balme, A. Belbel, F. Lalam, Glass Phys. Chem. 45, 503 (2019); <https://doi.org/10.1134/S1087659619060087>
- [26]A.A. Abul-Magd, H.Y. MorshidyA.M. Abdel-Ghany, Opt. Mater. 109,110301 (2020); <https://doi.org/10.1016/j.optmat.2020.110301>
- [27]N.R. Noori, R.S. Mamoori, P. Alizadeh, A. Mehdikhani, J. Ceram. Process Res.9,246 (2008).
- [28]F.G. Correa, J.B. Martínez, Mater. Sci. Pol. 32,682 (2014); <https://doi.org/10.2478/s13536-014-0250-9>
- [29]J.C. Hwan, P.J. Yeon, J. Ceram. Process. Res. 11,698 (2010).
- [30]M. El-Kemary, N. Nagy, I. El-Mehasseb, Mat. Sci. Semicon. Proc.16,1747 (2013); <https://doi.org/10.1016/j.mssp.2013.05.018>
- [31]Y. Wu, Y. He, T. Wu, T. Chen, W. Weng, Mater. Lett.61,3174 (2007); <https://doi.org/10.1016/j.matlet.2006.11.018>
- [32]S. Bale, S. Rahman, A. Awasthi, V. Sathe, J. Alloys Compd.460,(6992008).
- [33]B.N. Meera, A.K. Sood, N. Chandrabhas, J. Ramakrishna, Non-Cryst. Solids126,224 (1990); [https://doi.org/10.1016/0022-3093\(90\)90823-5](https://doi.org/10.1016/0022-3093(90)90823-5)
- [34]P. Narwal, M.S. Dahiya, A. Yadav, A. Hooda, A. Agarwal, S. Khasa, J. Non-Cryst. Solids498,470 (2018); <https://doi.org/10.1016/j.jnoncrysol.2018.01.042>
- [35]R.M.M. Morsi, S. Ibrahim,M.M. Morsi, Ceram. Int. 43,8306 (2017); <https://doi.org/10.1016/j.ceramint.2017.03.166>
- [36]E. Haily, L.A. Bih, Bouari, A. El Lahmar, M. El Marssi, B. Manoun, J. Aust. Ceram. Soc. 56,1467(2020); <https://doi.org/10.1007/s41779-020-00473-1>
- [37]V. Sharma, S.P. Singh, G.S. Mudahar, K.S. Thind, New J. Glass Ceram.2,128 (2012); <https://doi.org/10.4236/njgc.2012.24022>
- [38]S.P. Singh, R.P.S. Chakradhar, J.L. Rao, B. Karmakar, J. Alloys Compd.493,256 (2010).
- [39]A El-Taher, HMH Zakaly, M Pyshkina, EA Allam, RM El-Sharkawy, Mohamed E Mahmoud, Mohamed AE Abdel-Rahman.Zeitschrift für anorganische und allgemeine Chemie 647 (10), (2021) 1083-1090.(2021); <https://doi.org/10.1002/zaac.202100062>
- [40]Hesham MH Zakaly, Ahmed Ashry, Atef El-Taher, Adel GE Abbady, Elhassan A Allam, Rehab M El-Sharkawy, Mohamed E Mahmoud., Radiation Physics and Chemistry, 188, 109667.(2021); <https://doi.org/10.1016/j.radphyschem.2021.109667>
- [41]D.R. Lide, G. Baysinger, TeamLRN CRC Handbook of Chemistry and Physics.
- [42]S. Wang, K. Liang, J. Non-Cryst. Solids 354,1522 (2008); <https://doi.org/10.1016/j.jnoncrysol.2007.08.031>
- [43]V.K., Arun, Fundamentals of Inorganic Glasses, New York, (1994).
- [44]M. Saad, M. Poulain, J. Mater. Sci. Forum.19/20,11 (1987); <https://doi.org/10.4028/www.scientific.net/MSF.19-20.11>